

Inferior survival for patients with malignant peripheral nerve sheath tumors defined by aberrant *TP53*

Running title: *TP53* aberrations in malignant peripheral nerve sheath tumor

Maren Høland,^{1,2} Matthias Kolberg,¹ Stine Aske Danielsen,¹ Bodil Bjerkehagen,^{3,4} Ina A. Eilertsen,¹ Merete Hektoen,¹ Nils Mandahl,⁷ Eva van den Berg,⁸ Sigbjørn Smeland,^{2,6} Fredrik Mertens,⁷ Kirsten Sundby Hall,⁶ Piero Picci,⁵ Anita Sveen,¹ Ragnhild A. Lothe^{1,2}

¹Department of Molecular Oncology, Institute for Cancer Research, Oslo University Hospital, Oslo, Norway; ²Institute for Clinical Medicine, University of Oslo, Oslo, Norway; ³Department of Oral Biology, University of Oslo, Oslo, Norway; ⁴Department of Pathology, Division of Laboratory Medicine, Oslo University Hospital, Oslo, Norway; ⁵Laboratory of Experimental Oncology, Istituto Ortopedico Rizzoli, Bologna, Italy; ⁶Department of Oncology, Division of Cancer Medicine, Oslo University Hospital, Oslo, Norway; ⁷Department of Clinical Genetics, University and Regional Laboratories, Lund University, Lund, Sweden; ⁸Department of Genetics, The University Medical Center Groningen, The Netherlands

Corresponding Author: Ragnhild A. Lothe, PO Box 4950 Nydalen, NO-0424 Oslo, Norway. Phone: +47 2278 1728; Fax: +47 2278 1745. E-mail: rlothe@rr-research.no.

Key words: *TP53*; *MDM2*; malignant peripheral nerve sheath tumor; neurofibromatosis type 1; prognosis

Abstract

Malignant peripheral nerve sheath tumor is a rare and aggressive disease with poor treatment response, mainly affecting adolescents and young adults. Few molecular biomarkers are used in the management of this cancer type, and although *TP53* is one of few recurrently mutated genes in malignant peripheral nerve sheath tumor, the mutation prevalence and corresponding clinical value of the *TP53* network remain unsettled. We present a multi-level molecular

study focused on aberrations in the TP53 network in relation to patient outcome in a series of malignant peripheral nerve sheath tumors from 100 patients and 38 neurofibromas, including *TP53* sequencing, high-resolution copy number analyses of *TP53* and *MDM2*, and gene expression profiling. Point mutations in *TP53* were accompanied by loss of heterozygosity, resulting in complete loss of protein function in 8.2% of malignant peripheral nerve sheath tumors. Another 5.5% had *MDM2* amplification. *TP53* mutation and *MDM2* amplification were mutually exclusive and patients with either type of aberration in their tumor had a worse prognosis compared to those without (hazard ratio for 5-year disease-specific survival 3.5, 95% confidence interval 1.78-6.98). Both aberrations had similar consequences on the gene expression level, as analyzed by a *TP53*-associated gene signature, a property also shared with copy number aberrations and/or loss of heterozygosity at the *TP53* locus, suggesting a common “*TP53* mutated phenotype” in as many as 60% of the tumors. This was a poor prognostic phenotype (hazard ratio=4.1, confidence interval:1.7-9.8), thus revealing a *TP53*-non-aberrant patient subgroup with a favorable outcome. The frequency of the “*TP53* mutated phenotype” warrants explorative studies of stratified treatment strategies in malignant peripheral nerve sheath tumor.

Introduction

Malignant peripheral nerve sheath tumor is a rare and highly aggressive malignancy with a 5-year survival rate lower than 50%.¹ About half of the cases arise in individuals with neurofibromatosis type 1, while the remaining tumors are sporadic. The neurofibromatosis type 1 syndrome, caused by an inherited or *de novo* mutation in the tumor suppressor gene *NF1*, is one of the most common autosomal dominant disorders, with an incidence of 1 in 2,500-3,000 individuals.² The syndrome affects men and women equally, and the carriers have a 6-13% life time risk of developing malignant peripheral nerve sheath tumor.^{2, 3}

Malignant peripheral nerve sheath tumors typically have numerous DNA copy number aberrations, including deletions of *CDKN2A* and *NF1*, and gains of *EGFR*, *TOP2A*, and *BIRC5*.⁴⁻¹² Like malignant melanomas, malignant peripheral nerve sheath tumors are derived from cells of the neural crest lineage, and both malignant peripheral nerve sheath tumors and melanomas exhibit constitutive activation of RAS signaling, mainly through *NF1* or *BRAF* mutations, respectively. However, while melanomas have a high genome-wide mutation frequency,¹³ malignant peripheral nerve sheath tumors typically have few mutations at the nucleotide level.^{14, 15} Recurrent mutations in malignant peripheral nerve sheath tumors have only been found in a handful of genes, including *NF1*, *TP53*, *TERT*, *SUZ12*, *EED* and *SPTBN2*.¹⁴⁻¹⁹

The importance of aberrations in the tumor suppressor gene *TP53* in cancer has been widely documented. In fact, the TP53 network has been suggested to be dysfunctional in most human tumors.²⁰ In malignant peripheral nerve sheath tumor, the first *TP53* point mutation was reported in a patient with neurofibromatosis type 1 in 1989.²¹ A decade later, two independent laboratories found that concurrent knockout of one allele of each of the two genes *NF1* and *TP53* in mouse models resulted in the formation of tumors similar to malignant peripheral nerve sheath tumors.^{22, 23} These tumors developed when the mutated alleles were located on the same chromosome (in *cis*), followed by loss of the remaining copy of chromosome 17, and resulting in loss of heterozygosity and complete loss of function of both gene products. Today, more than 30 articles on *TP53* mutations in malignant peripheral nerve sheath tumors have been published (**Table 1** and **Supplementary Table S1**). Still the prevalence and clinical impact of *TP53* mutations in malignant peripheral nerve sheath tumor remain inconclusive, due to the limited number of samples available for analyses of this rare cancer type.

In addition to aberrations targeting the *TP53* gene itself, the TP53 network can be dysregulated by changes in several other genes, including amplification of *MDM2* or inactivating alterations of *CDKN2A*.²⁰ MDM2 promotes tumor formation by targeting TP53 for proteasomal degradation, and *CDKN2A* encodes two distinct tumor suppressor proteins, p14^{ARF} and p16^{INK4a}, both acting to induce cell cycle arrest; the p14^{ARF} isoform interacts with and sequesters MDM2, thereby stabilizing TP53.²⁴

In this study, we analyzed genomic aberrations of *TP53* and *MDM2* in relation to clinical end-points in a series of more than 100 malignant peripheral nerve sheath tumors from patients with and without neurofibromatosis type 1. For interpretation of the down-stream effects of the various genomic aberrations in the TP53 network, we analyzed a *TP53*-mutant signature at the gene expression level.

Materials and Methods

Literature survey

A search on NCBI PubMed²⁵ was performed to capture articles that included analyses of *TP53* mutations in malignant peripheral nerve sheath tumors (**Figure 1**), and a detailed overview of the identified publications, the methods used, and the specific *TP53* mutations found in these studies, are given in **Table 1** and **Supplementary Table S1**.

Patients and samples

The included patients were treated between 1980 and 2010 at four European sarcoma centers: the Norwegian Radium Hospital, Oslo, Norway; Skåne University Hospital, Lund, Sweden; the University Medical Centre of Groningen, The Netherlands; and the Istituto Ortopedico Rizzoli, Bologna, Italy. The sample biobanks and research protocols were approved by the regional/local ethics committees of each participating country, following informed consent

from the patients. The multicenter samples and protocols used in the present study were approved by the Regional Committee for Medical and Health Research Ethics, South East Norway [2010/223/REKsør-øst].

Malignant peripheral nerve sheath tumors were collected from 50 patients with sporadic disease (median age at diagnosis 48 years) and 50 patients with neurofibromatosis type 1 (median age 29 years). None of the malignant peripheral nerve sheath tumors were radiation-induced, two were malignant triton tumors. In total, 143 tumor samples have been investigated, including 105 malignant peripheral nerve sheath tumors from 100 patients and 38 neurofibromas, of which different subsets were included in different analyses, based on the available material and sample types. Blood samples were available from 18 malignant peripheral nerve sheath tumor patients. The clinical data are summarized in **Table 2**, while **Supplementary Tables S2** and **S3** provide an overview of clinical and molecular data for individual malignant and benign tumors, respectively.

The malignant peripheral nerve sheath tumor diagnoses were determined by sarcoma pathologists at specialized sarcoma centers in each country, and all tumors were diagnosed according to established criteria.²⁶ In addition, neighboring tissue sections of all frozen tumor samples used for DNA and RNA extraction were morphologically evaluated, and the tumor cell percentage was visually estimated to a median of ~100% (interquartile range: 10%).

Despite their limitations in sensitivity and specificity for diagnosis of malignant peripheral nerve sheath tumor, S100 and SOX10 are markers of neural crest differentiation.²⁷ From gene expression data we observed, in agreement with previous publications,^{27,28} lower expression of both S100B and SOX10 in malignant peripheral nerve sheath tumors compared to neurofibromas ($P=3 \times 10^{-8}$ and $P=3 \times 10^{-8}$ respectively, Mann–Whitney–Wilcoxon, Supplementary Figure S5a-b), although a few malignant tumors have expression at the level

of the benign tumors (Supplementary Figure S5c). The expression of S100A1 was low in both the malignant peripheral nerve sheath tumors and the benign neurofibromas (Supplementary Figure S5d), supporting no inclusion of erroneously diagnosed malignant melanomas.²⁹

Loss of trimethylation of lysine 27 of histone H3 (H3K27m3) has been found to discriminate malignant peripheral nerve sheath tumors from benign neurofibromas (Supplementary Figure S6a).^{30, 31} We used gene set enrichment analyses to evaluate loss of H3K27m3 in our tumor material (**Supplementary Table S2, S3, and S7**). In agreement with previous publications,^{30, 31} we found that the malignant tumors had significantly higher gene set scores, and therefore expectedly a higher degree of H3K27m3 loss than the benign neurofibromas ($P= 0.0009$, Mann–Whitney–Wilcoxon, **Supplementary Figure S6b**), further supporting the true malignant peripheral nerve sheath tumor diagnoses.

DNA and RNA isolation

Two different methods were used for DNA and RNA isolation. Either the tumor tissue was homogenized using TissueRuptor, and DNA and RNA was extracted using the Allprep DNA/RNA/miRNA Universal Kit as recommended by the manufacturer (QIAGEN, Hilden, Germany), or the tumor tissue was manually ground in liquid nitrogen using a mortar and pestle before separate isolation of RNA and DNA. DNA was extracted using a semi-automatic phenol-chloroform extraction method followed by ethanol precipitation in a 340A Nucleic Acid Extractor (Applied Biosystems, Foster City, CA, USA), while RNA was isolated from the tissue samples by standard Trizol methodology in 1 ml Trizol (Invitrogen, Carlsbad, CA, USA), followed by phase separation by chloroform and precipitation using 2-propanol. The RNA pellets were dissolved in RNase free water at 55 °C. Quantity and quality measurements were carried out using UV spectrometry (NanoDrop ND-1000, Thermo Fisher

Scientific, Waltham, MA, USA) and Agilent 2100 Bioanalyzer (Agilent Technologies, Santa Clara, CA, USA). All RNA samples had a RIN value above 6 (average 8.5).

Mutation analyses

The full coding sequence of *TP53*, exons 2-11 (393 codons, Ensembl transcript TP53-001 [ENST00000269305.4], human assembly GRCh37) and the flanking intronic regions (10 bases downstream and upstream of the exons), was analyzed for mutations by Sanger sequencing. Genomic *TP53* sequences were amplified from the DNA extracts in separate singleplex (exons 2-4, exons 5-6 and exons 7-9) and multiplex (exon 10 and 11) PCR reactions giving rise to five distinct DNA fragments. HotStarTaq DNA Polymerase or QIAGEN Multiplex PCR Kit was used as recommended by the manufacturer (Qiagen, Hilden Germany). The PCR program included 35 cycles, an annealing temperature of 60°C, and a 45 or 90 second elongation step for the singleplex or multiplex PCR reaction, respectively. The PCR products were subjected to enzymatic purification using illustra ExoProStar 1-Step kit (GE Healthcare Life Sciences, Marlborough, MA, United States) and sequencing of the purified products was performed for seven distinct fragments (exons 2-3, 4, 5-6, 7, 8-9, 10, and 11) using the BigDye Terminator v3.1 Cycle Sequencing Kit (Applied Biosystems™, ThermoFisher Scientific, Waltham, MA, USA). Details for the primers used in the initial PCR amplification and the sequencing reaction are listed in **Supplementary Table S4**. The resulting sequence products were further purified using the BigDye XTerminator® Purification Kit (Applied Biosystems™) and subjected to sequencing using the 3730 DNA Analyzer (Applied Biosystems™). *In silico* analysis of mutations was performed manually by two investigators using the Sequencing Analysis (v5.3.1, Applied Biosystems™) and SeqScape (v2.5.0, Applied Biosystems™) software's. All detected mutations were confirmed

by sequencing of a new independent PCR product. The bases of the *TP53* sequence were reported according to the sequence of the gene, hence the reverse genomic DNA strand.

DNA copy number analysis

DNA from fresh frozen tumor samples, 91 malignant peripheral nerve sheath tumors and 28 neurofibromas, and 18 blood samples were individually processed and hybridized on Genome-Wide Human SNP Array 6.0 from Affymetrix (Thermo Fisher Scientific) as described in the Affymetrix Cytogenetics Copy Number Assay User Guide (P/N 702607 Rev. 2). Raw probe intensity data from scanned images of the arrays were stored in cell intensity files by the Affymetrix Gene Chip Command Console software (version 1.0), and quality control of the individual cell intensity files was performed using the Affymetrix Genotyping Console software (version 4.1.4.840). All samples had a cell intensity data quality above the recommended threshold (Contrast QC > 0.4) for individual samples, and >1.7 for the dataset (Affymetrix white paper; Quality Control Assessment in Genotyping Console, September 30, 2008, Revision 1) and a Median Absolute Pairwise difference below 0.4 (Affymetrix white paper; Median of the Absolute Values of all Pairwise Differences and Quality, Control on the Affymetrix, Genome-Wide Human SNP Array 6.0, February 11, 2008, Revision 1).

For copy number analysis the cell intensity files were preprocessed according to the PennCNV protocol³² adapted for Affymetrix genotyping arrays,³³ as previously described.³⁴ HapMap samples previously analyzed on the SNP Array 6.0 (n = 270 individuals from four populations)³⁵ were used as reference for quantile normalization and calculation of Log R Ratio and B Allele Frequency.

Allele-specific copy number analysis was performed on the Log R Ratio and B Allele Frequency values using the ASCAT algorithm (ASCAT version 2.3, penalty parameter 50).³⁶

Discrete copy number states were decided relative to the median genome wide copy number in each tumor sample. All genomic positions refer to genome version GRCh37 (Hg19).

For genomic identification of significant targets in cancer (GISTIC analysis)^{37, 38} the Log R Ratio values were subjected to winsorization and single-sample segmentation by the PCF algorithm implemented in the Bioconductor package copynumber (version 1.12.0; penalty parameter $\gamma = 100$; minimum number of probes per segment, $k_{min} = 5$).³⁹ Version 2.0.22 of GISTIC was used, and copy number estimates >0.1 were called as copy number gain while estimates <-0.1 were called as loss, the broad length cut-off was set to 0.7 (`-brlen 0.7`), normal arbitrated peel-off was performed (`-armpeel 0`) and we calculated the significance of deletions at a gene level (`-genegistic 1`), otherwise default settings. The reference genome file `hg19.mat` and the copy number variation file `CNV.hg19.bypos.111213.txt` were used.

Gene expression analysis

Total RNA (100 ng) from 63 malignant peripheral nerve sheath tumors and 15 neurofibromas was used as input for cDNA synthesis, followed by amplification and DNA sense strand labeling according to the GeneChip Whole Transcript (WT) PLUS Reagent Kit Manual (Affymetrix). Each sample was hybridized to Affymetrix GeneChip Human Transcriptome 2.0 arrays for 16 hours and washed, stained and scanned as recommended. For each sample, a cell intensity file was generated by the Affymetrix GeneChip Command Console software (version 4.0). The cell intensity files intensities were adjusted by guanine cytosine count correction and signal space transformation before being further processed through background correction, quantile normalization and summarization at the gene level by robust multiarray average using the Affymetrix Expression Console Software (v1.4.1.46, HTA-2_0.r3 library files), giving data on log₂ scale. All samples passed the recommended quality

control measures and no outlier samples were identified. The hta-2_0-na36.hg19_transcript.csv file from Affymetrix was used for transcript cluster annotation. The dataset was filtered to include only protein-coding transcripts and entries from the NCBI Reference Sequence Database (RefSeq) were prioritized in order to retain one transcript cluster per gene. Gene expression data on 18,618 unique genes was used as input for single-sample gene set expression enrichment analysis using the Bioconductor package GSVA (version 1.22.4, default settings).⁴⁰

Statistical analysis

Five-year disease-specific survival was analyzed using the software package IBM SPSS version 21.0 (IBM Corporation, Armonk, NY, U.S.A.). The Kaplan-Meier method and the Cox proportional hazards model with Wald test were used to provide univariable and multivariable hazard-ratios and 95% confidence intervals. In multivariable analyses, all variables were included in the proportional hazards model. Only patients with a primary malignant peripheral nerve sheath tumor, or a local relapse, were included in the survival analyses (**Table 3** and **Supplementary Table S2**). Five-year disease specific survival was counted from the time of diagnosis of the primary malignant peripheral nerve sheath tumor and considering death from disease as an event. All survival analyses were also performed separately for the primary and the relapsed malignant peripheral nerve sheath tumors and the same associations as for the primaries and relapses combined were found (data not shown).

Fisher's exact test was used to compare the frequency distributions between groups, Mann-Whitney-Wilcoxon exact test was used to compare differences in the distribution between two groups of continuous variables, and Spearman's test were used to analyze correlation for continuous and ordinal variables. All tests were 2-sided, and *P*-values lower than 0.05 are reported as significant.

Results

Literature survey indicates a moderate mutation prevalence of *TP53* in malignant peripheral nerve sheath tumor

Across the 31 published papers found to report *TP53* mutations in malignant peripheral nerve sheath tumor (including the present study and excluding two studies on patients with the Li-Fraumeni syndrome), the *TP53* mutation prevalence was 16.8% (78/464 tumors from unique patients, **Table 1** and **Supplementary Table S1**). By excluding samples reported to be formalin-fixed and paraffin-embedded, the mutation prevalence dropped to 13.7% (43/314 tumors), compared to 23% (35/150 tumors) for formalin-fixed samples alone.

Totally 85 *TP53* mutations were identified in malignant peripheral nerve sheath tumors in the present study and the reviewed literature, including double mutations in 3 tumors and 4 mutations found in patients with the Li-Fraumeni syndrome. These represent 73 unique mutations in 62 different codons of exons 4 to 9, or in intronic sequences (**Figure 2a-c**). The mutation types and distribution resemble those reported for other tumor types (**Supplementary Figure S1**, data on somatic mutations from the IARC *TP53* Database),⁴¹ and the most recurrent mutation in malignant peripheral nerve sheath tumors (p.R175H, identified in four tumors) is also one of the most recurrent mutations in cancer in general. However, the percentage of *TP53* splice site mutations in malignant peripheral nerve sheath tumors was higher than in cancer in general, 8.2% versus 2.3% respectively.

Only the mutated allele of *TP53* remains

Among our own 98 malignant peripheral nerve sheath tumor patients we identified nine *TP53* point mutations in eight tumors from eight different patients (8.2%), while no *TP53* mutations were identified in 35 benign tumors (**Supplementary Table S2 and S3**). Only two of the identified mutations have been reported in malignant peripheral nerve sheath tumors

previously (p.S241F and p.R273H, **Supplementary Table S1**), although all have been reported in other cancers (TP53 database⁴¹). The mutation types included one nonsense, one splice site, and seven missense mutations (**Figure 2a-c**). The nonsense mutation has been reported by IARC to affect tetramerization of the TP53 protein, while the splice site mutation is found at a consensus acceptor splice site and should affect mRNA processing. All the missense mutations have been reported to be deleterious to protein function, except for the p.V203L mutation.⁴¹ However, this p.V203L mutation was found as a double mutant along with the deleterious p.V197E mutation in one primary malignant peripheral nerve sheath tumor. The Sanger sequencing chromatograms (**Supplementary Figure S2**) indicated that all mutations, except p.V203L, were hemi- or homozygous, with little, or nothing of the wild-type allele present.

Allele-specific copy number data confirmed that all *TP53* mutated samples were homo- or hemizygous for all single nucleotide polymorphism probes in a region surrounding the *TP53* locus. This supports the notion that loss of heterozygosity, either by loss or copy number neutral loss of heterozygosity, has resulted in complete loss of function of the *TP53* gene in all mutated tumors.

Polymorphisms in *TP53*

The common non-synonymous single nucleotide polymorphism in codon 72 of exon 4 in *TP53* (c.215G>C, p.R72P, rs1042522) was also examined in the Sanger sequencing data, and 15 malignant peripheral nerve sheath tumors were regarded as homozygous C/C allele carriers, 24 as heterozygous and 58 as homozygous G/G carriers (**Supplementary Table S2**). The calculated G allele frequency across malignant peripheral nerve sheath tumors from 97 patients was 72% (considering heterozygous samples as 50% C and G

$(n_{(C/G)}+2n_{(G/G)})/2n_{(Total)}$), in good concordance with the European (non-Finnish) samples included in the Exome Aggregation Consortium database.⁴²

We also identified less common intragenic single nucleotide polymorphism variants (**Figure 2** and **Supplementary Tables S2** and **S3**), including c.639A>G^{p.R213R} (rs1800372) in five malignant peripheral nerve sheath tumors and one neurofibroma, as well as c.108G>A^{p.P36P} (rs1800370) and c.993+12T>C (rs1800899) found in overlapping samples, including three malignant tumors from two patients and two neurofibromas.

Increased mutation frequency by integration of copy number aberrations and LOH at the *TP53* locus

Copy number aberration and zygosity at the *TP53* locus were analyzed in malignant peripheral nerve sheath tumors from 91 patients (**Figure 2d** and **Supplementary Table S2**), and loss of one or two copies of the gene was found in 30 malignant tumors (33%); however, because almost half of the tumors had a median genome-wide copy number of 3 or higher, none of these tumors had complete loss of the *TP53* gene. Point mutations co-occurred with copy number loss in four patients. Of the 30 malignant peripheral nerve sheath tumors with loss, 20 were neurofibromatosis type 1 associated and 10 were sporadic cases ($P=0.044$, Fisher's exact test, $n=91$). For tumors with copy number gain ($n=9$, 10%), the affected region was not limited to the *TP53* gene sequence, but included all or most of chromosome 17, suggesting that *TP53* was not a specific target gene for these aberrations. loss of heterozygosity at the *TP53* locus was found in 40 (44%) malignant peripheral nerve sheath tumors, of these 12 cases (13%) were copy number neutral which co-occurred with point mutations in three cases. Altogether, malignant peripheral nerve sheath tumors from 51 patients (57%) had genetic aberrations in *TP53* (point mutation and/or copy number aberration). These *TP53* copy number changes were found to be tumor-specific, as no

aberrations were found in 18 blood samples from malignant peripheral nerve sheath tumor patients, nor in 28 neurofibromas.

Amplification of the *MDM2* locus affects malignant peripheral nerve sheath tumors with non-aberrant *TP53*

Five of the 91 malignant peripheral nerve sheath tumors had amplification of the *MDM2* gene (defined as gain of five or more copies) (**Figure 2d**). *MDM2* amplification and *TP53* point mutations were mutually exclusive, while *MDM2* amplification and loss of the *TP53* locus were nearly mutually exclusive (co-occurrence in one tumor). GISTIC analysis³⁸ showed that *MDM2* (chr12:69127775-69649624; q -value= 1.32×10^{-5}) and *TP53* (chr17:7,479,693-7,613,707; q -value=0.075) were contained within focal regions with aberrant and frequent gains and losses in malignant peripheral nerve sheath tumors, respectively, suggesting that *MDM2* and *TP53* were the possible target genes for the copy number aberrations. No malignant peripheral nerve sheath tumors had amplification of the *MDM4* gene, a homolog of *MDM2*.

Poor prognostic associations of genetic aberrations in *TP53* and *MDM2*

For patients with sporadic malignant peripheral nerve sheath tumor point mutation in *TP53* was associated with a higher age at diagnosis ($P=0.01$, Mann–Whitney–Wilcoxon test), with a median age of 71 years for patients with mutation ($n=5$) versus 43 years for patients without mutation ($n=44$), this association was not found for the neurofibromatosis type 1 patients.

TP53 mutation was associated with a poor survival for the complete patient group, and all patients with mutation died of the disease within five years (median time to death 19 months), compared to 49% (median time to death 42 months) of patients without mutation (hazard ratio=3.2, confidence interval: 1.44-6.88, $P=0.04$, $n=84$, **Supplementary Figure S3a**).

Combined analysis of *TP53* mutation and *MDM2* amplification data revealed an even

stronger prognostic impact, independent of clinical parameters in multivariable analysis (**Table 3**). Moreover, a total of 60% of the patients (53/89, **Figure 2d**) had a genetic aberration in either *TP53* (point mutations, copy number aberration and/or loss of heterozygosity) or *MDM2* (amplification) and this was significantly associated with an inferior 5-year disease specific survival rate (**Figure 3a** and **Supplementary Figure S3a-e**). The same association was observed for patients believed to be in complete remission after surgery (n=57) (**Figure 3b**), and in separate analyses of neurofibromatosis type 1 associated and sporadic cases (**Supplementary Figure S3g-h**).

There was also an association between the single nucleotide polymorphism at codon 72 of *TP53* (c.215G>C, p.R72P) and patient survival (**Supplementary Figure S3f**), and the single nucleotide polymorphism was an independent prognostic marker in multivariable analysis including clinical parameters (neurofibromatosis type 1 association, sex, age at diagnosis, primary tumor size and location, and complete remission status). Compared to the homozygous G/G allele carriers (n=43), the heterozygous (G/C) allele carriers (n=20) had a reduced risk of dying of the disease (multivariable hazard ratio=0.49, confidence interval: 0.19-1.26, $P=0.14$), while the homozygous C/C allele carriers (n=8) had a significantly higher risk (multivariable hazard ratio=2.7, confidence interval: 1.02-7.128, $P=0.046$). We found an association between the codon 72 polymorphism and the genetic aberrations found in *TP53* ($P=0.003$, Fisher's exact test, n=88), where 93% (13/14) of tumors homozygous for C were affected by aberration in *TP53* (point mutations, copy number aberration and/or loss of heterozygosity), compared to 55% (29/53) of the tumors homozygous for G and 38% (8/21) of the heterozygous tumors.

For the less common single nucleotide polymorphism variants, c.639A>G^{p.R213R}, c.108G>A^{p.P36P}, and c.993+12T>C, there were no association with prognosis.

Genetic aberrations define a common, poor prognostic “TP53 mutated phenotype” at the transcriptome level

The genomic aberrations of *TP53* and *MDM2* were analyzed in relation to gene expression data in 63 malignant peripheral nerve sheath tumors and 15 neurofibromas to reveal the transcriptional consequences on the TP53 network. As anticipated, the *TP53* expression level was lower in tumors with copy number loss of the *TP53* gene (n=14) compared to tumors without loss (n=42) (difference in median on log₂-scale=0.8, $P=0.01$, Mann–Whitney–Wilcoxon test), and tumors with *TP53* mutation (n=4) did not have a significantly different *TP53* expression level than tumors without mutation (n=56, **Supplementary Figure S4a**). *MDM2* gene expression was positively correlated with the discrete copy number of the *MDM2* gene (Spearman’s rho=0.51, $P=3\times 10^{-5}$, n=60, **Supplementary Figure S4b**), and a particularly high expression was found in tumors with high-level amplification. Furthermore, *TP53* and *MDM2* gene expression were positively correlated (Spearman’s rho=0.30, $P=0.007$, n=63, **Supplementary Figure S4c**), however in contrast to *TP53*, *MDM2* gene expression was significantly lower in *TP53* mutated (n=4) compared to wild-type tumors (n=58) (difference in median on log₂-scale=1.71, $P=0.002$, Mann–Whitney–Wilcoxon test, **Supplementary Figure S4d**).

We performed single-sample gene set expression enrichment analysis for a set of 15 genes previously found to be upregulated in breast tumors with point mutations in the *TP53* gene (**Supplementary Table S5**).⁴³ Significant associations were found between the gene set scores and genetic aberrations, with highest scores in samples with *TP53* point mutation or *MDM2* amplification, followed by copy number aberration and/or loss of heterozygosity at the *TP53* locus, thus indicating a common “TP53 mutated phenotype” resulting from either type of genomic aberration (**Figure 3c-e**). Moreover, neurofibromas (n=15), none of which

had genetic aberrations in these two genes, had significantly lower gene set scores than the malignant tumors (n=63) ($P=3 \times 10^{-10}$, Mann–Whitney–Wilcoxon test). For malignant peripheral nerve sheath tumors without genetic aberrations in *TP53* or *MDM2*, there was a trend that those with loss of the *CDKN2A* gene (n=15) had a higher gene set score than those without loss (n=13) ($P=0.11$, Mann–Whitney–Wilcoxon test).

Gene expression of *TP53* or *MDM2* alone was not associated with patient survival; however, the gene set analysis confirmed the prognostic relevance of the TP53 network, with increasing risk according to a continuously increasing TP53 gene set score (hazard ratio=4.1, confidence interval: 1.73-9.79, $P=0.001$, n=60). There was a bimodal distribution of the gene set score across the samples, and stratification of the patients (**Figure 3e-f**) revealed a 5-year disease specific survival rate of 39%, for the high-score group compared to 75% for the low-score group ($P=0.01$). This prognostic relevance was retained among the subset of patients who were in complete remission (hazard ratio=4.4, confidence interval: 1.57-12.1, $P=0.005$, n=48).

By estimating PRC2 loss using gene set enrichment analyses we confirm that loss of H2K27m3 is associated with inferior survival for malignant peripheral nerve sheath tumor patients (**Supplementary Figure S6c**). However, in multivariable analyses, the TP53 gene set signature had the strongest prognostic impact (**Supplementary Figure S6e**), and dysregulation of both biological processes identified a patient subgroup (n=25, 42%) with a particularly poor survival (hazard ratio=9.1, confidence interval:2.07-39.9, $P=0.003$, **Supplementary Figure S6d**).

Discussion

TP53 is one of few recurrently mutated genes in malignant peripheral nerve sheath tumor. Here, we report the largest study on genomic aberrations in *TP53* and its negative regulator

MDM2 published to date for this cancer type. We confirm that point mutations in *TP53* and amplification of *MDM2* are mutually exclusive; but while each of these aberrations have moderate frequency alone, integrated gene expression analyses reveal a common and poor prognostic “TP53 mutant phenotype” in 60% of the patients.

The survey of the literature on *TP53* mutations in malignant peripheral nerve sheath tumors revealed a mutation prevalence of 16.8% across 464 tumors (**Table 1**), clearly establishing that *TP53* mutated tumors constitute a significant subgroup of malignant peripheral nerve sheath tumors. In our own patient cohort, we found mutations in 8.2%. The higher prevalence found in the literature may in part be explained by the inclusion of mutation data from formalin fixed and paraffin embedded samples, which are known to give rise to higher numbers of false positive mutation calls. Furthermore, the literature overview contains several single case reports with *TP53* mutated tumors, suggesting that case reports with wild-type samples are underrepresented. However, excluding studies with a small sample size did not have a profound effect on the overall mutation prevalence.

All mutated tumors had loss of heterozygosity at the *TP53* locus, indicating that biallelic inactivation of *TP53* is an important event in a subgroup of malignant peripheral nerve sheath tumors. However, consistent with our previous results,⁴⁴ such events are rare. The dominant negative effect of *TP53* mutation may indicate that biallelic inactivation is redundant to the malignant cells. A high percentage of *TP53* mutations in malignant peripheral nerve sheath tumors, and in cancer in general, are missense mutations in exons 4 to 9 that affect the DNA binding domain and create full-length protein subunits that can form non-functional wild-type/mutant heterotetramers. However, as stated by Rivlin and colleagues,⁴⁵ the heterozygous state is often transient, and *TP53* mutations are frequently followed by loss of heterozygosity

during cancer progression, implying that the dominant negative effect is not sufficient to inactivate the wild-type protein.

We found that one third of malignant peripheral nerve sheath tumors had loss of a chromosomal region containing *TP53* as a possible gene target, as determined by GISTIC analysis. However, no tumors had complete deletion of the *TP53* locus, in good concordance with the study by Lee *et al.*¹⁴ As others have also suggested previously,^{46, 47} our data imply that haploinsufficiency of *TP53* also contributes to malignant peripheral nerve sheath tumor formation. Studies in other cancer types have shown *TP53* methylation as a mechanism for allele inactivation,⁴⁸⁻⁵¹ however, methylation of *TP53* in malignant peripheral nerve sheath tumor has so far not been identified.^{46, 52} Furthermore, in mouse models one mutated *Tp53* allele, in combination with mutation in the *Nf1* gene, trigger malignant peripheral nerve sheath tumor development.^{22, 23, 47} Only 20% of malignant peripheral nerve sheath tumors with loss of heterozygosity at the *TP53* locus were shown to have a mutation in the remaining allele. In most cases, the loss of heterozygosity region included the whole chromosome arm, and therefore, *TP53* cannot be singled out as the main target for these changes. Nevertheless, we observed a poorer prognosis for patients with loss of heterozygosity of the *TP53* locus in their tumors.

As shown in the current and previous studies, a subgroup of malignant peripheral nerve sheath tumors without *TP53* mutation had amplification of the *MDM2* gene.^{53, 54} Tumors with mutation in *TP53* also had lower expression of *MDM2*, which underlines the mutually exclusive effect of these genetic events. In total, 60% of the patients had aberrations in either *TP53* or *MDM2*, showing that the TP53 network is targeted in a much higher fraction of malignant peripheral nerve sheath tumors than can be explained by point mutations in *TP53* alone. Further highlighting the importance of the TP53 network, expression analysis of a

gene set previously found to be associated with *TP53* point mutation in breast tumors,⁴³ revealed a significant association with *TP53/MDM2* genetic aberrations also in malignant peripheral nerve sheath tumors. This suggests similar consequences of the different types of mutations at the transcriptome level and therefore a common “TP53 mutated phenotype”. The majority of the genes in this expression signature have been shown to have roles in cellular processes relevant for tumor development (cell cycle progression, apoptosis, DNA damage response), and the poor patient survival associated both with *TP53/MDM2* genetic aberrations and the gene expression signature reinforces a clinical importance of the “*TP53* mutated phenotype” in malignant peripheral nerve sheath tumor.

Loss of H3K27me3 has been found to differentiate malignant peripheral nerve sheath tumor from benign neurofibromas^{30, 31} and to identify a patient subgroup with poor survival.³¹ The Polycomb repressive complex 2 (PRC2) establishes and maintains the di- and trimethylation of H3K27, and it has been shown that malignant peripheral nerve sheath tumors with homozygous loss of PRC2 components have complete loss of H3K27me3.^{14, 15} Using gene set enrichment analyses, we found an inferior survival among malignant peripheral nerve sheath tumor patients with dysregulated PRC2 activity; nevertheless, the *TP53* gene set still added prognostic information and this signature was an even stronger predictor of survival than the PRC2 gene set.

Somatic or germline single nucleotide polymorphisms may affect the patients’ risk for developing a tumor or progression of the disease. Indeed, we and others have found that patients with a proline residue at codon 72 of *TP53* had worse outcome than patients with an arginine residue, or a heterozygous genotype.⁵⁵ The difference could be explained by the higher frequency of genetic aberrations in *TP53* (point mutations, copy number aberration and/or loss of heterozygosity) among the tumors with a codon 72 proline.

In malignant peripheral nerve sheath tumor cell lines we have observed,⁵⁶ as anticipated, that drugs targeting MDM2 induced proteasomal degradation of TP53, *e.g.* serdemetan and Nutlin-3, have little effect in *TP53* mutant cell lines, as compared to *TP53* wild-type cell lines and normal controls. However, we found that AZ3146, a drug against the protein kinase TTK, also known as MPS1 (Monopolar spindle 1), one of the genes in the 15-gene TP53 signature set, gave a moderate, but consistently higher effect in seven malignant peripheral nerve sheath tumor cell lines compared to bone marrow and normal Schwann cells. This suggests that TTK could be a target for treatment of the TP53 inactivated tumors, which also have a high expression of TTK (**Figure 3e**). TTK has been identified as a potential diagnostic, as well as prognostic, marker and as a target for therapy in several malignancies, including melanoma and glioblastoma.⁵⁷ A handful of clinical trials involving TTK inhibition have been conducted. Interestingly, one of these trials (ClinicalTrials.gov identifier NCT00676949) used peptide vaccines against TTK in combination with four other epitopes highly expressed in solid tumors, of which two were also related to the TP53 signature gene set, DEPDC1 and KIF20B (as KIF2C a member of the kinesin superfamily), and this clinical trial showed a significant association between the treatment and longer survival.⁵⁸

In conclusion, the survey of the literature and the findings from our own patient cohort confirm the importance of *TP53* point mutations in a subpopulation of malignant peripheral nerve sheath tumors. Integrated analysis with copy number aberrations and gene expression changes indicates that the TP53 network has an important role in an even higher proportion of tumors, translating into a clinically relevant patient subgroup with poor prognostic associations. There is currently no other curative therapy for malignant peripheral nerve sheath tumors than surgical resection,⁵⁹ and we suggest that the biological knowledge of a

prevalent “TP53 mutated phenotype” can be explored as a stratification parameter for novel treatments of this aggressive tumor type.

Acknowledgments

The authors are grateful to Mette Eknæs at the Department of Molecular Oncology (Oslo University Hospital) for excellent technical assistance.

Conflict of interest statement. The authors declare that they have no conflict of interest.

Funding: This study was supported by the Norwegian Cancer Society (project number 6824048-2016 to A. Sveen and project number 72190-PR-2006-0442 to R.A. Lothe), the Southern and Eastern Norway Regional Health Authority (R.A. Lothe), the foundation “Stiftelsen Kristian Gerhard Jebsen”, and the Research Council of Norway.

References

1. Kolberg M, Holand M, Agesen TH, *et al.* Survival meta-analyses for >1800 malignant peripheral nerve sheath tumor patients with and without neurofibromatosis type 1. *Neuro Oncol* 2013;15:135-47.
2. Evans DG, Huson SM, Birch JM. Malignant peripheral nerve sheath tumours in inherited disease. *Clin Sarcoma Res* 2012;2:17.
3. McCaughan JA, Holloway SM, Davidson R, *et al.* Further evidence of the increased risk for malignant peripheral nerve sheath tumour from a Scottish cohort of patients with neurofibromatosis type 1. *J Med Genet* 2007;44:463-6.
4. Berner JM, Sorlie T, Mertens F, *et al.* Chromosome band 9p21 is frequently altered in malignant peripheral nerve sheath tumors: studies of CDKN2A and other genes of the pRB pathway. *Genes Chromosomes Cancer* 1999;26:151-60.
5. Nielsen GP, Stemmer-Rachamimov AO, Ino Y, *et al.* Malignant transformation of neurofibromas in neurofibromatosis 1 is associated with CDKN2A/p16 inactivation. *Am J Pathol* 1999;155:1879-84.

6. Kourea HP, Orlow I, Scheithauer BW, *et al.* Deletions of the INK4A gene occur in malignant peripheral nerve sheath tumors but not in neurofibromas. *Am J Pathol* 1999;155:1855-60.
7. Lothe RA, Karhu R, Mandahl N, *et al.* Gain of 17q24-qter detected by comparative genomic hybridization in malignant tumors from patients with von Recklinghausen's neurofibromatosis. *Cancer Res* 1996;56:4778-81.
8. Mertens F, Dal Cin P, de Wever I, *et al.* Cytogenetic characterization of peripheral nerve sheath tumours: a report of the CHAMP study group. *J Pathol* 2000;190:31-8.
9. Skotheim RI, Kallioniemi A, Bjerkhagen B, *et al.* Topoisomerase-II alpha is upregulated in malignant peripheral nerve sheath tumors and associated with clinical outcome. *J Clin Oncol* 2003;21:4586-91.
10. Storlazzi CT, Brekke HR, Mandahl N, *et al.* Identification of a novel amplicon at distal 17q containing the BIRC5/SURVIVIN gene in malignant peripheral nerve sheath tumours. *J Pathol* 2006;209:492-500.
11. Holtkamp N, Malzer E, Zietsch J, *et al.* EGFR and erbB2 in malignant peripheral nerve sheath tumors and implications for targeted therapy. *Neuro Oncol* 2008;10:946-57.
12. Brekke HR, Ribeiro FR, Kolberg M, *et al.* Genomic changes in chromosomes 10, 16, and X in malignant peripheral nerve sheath tumors identify a high-risk patient group. *J Clin Oncol* 2010;28:1573-82.
13. Lawrence MS, Stojanov P, Polak P, *et al.* Mutational heterogeneity in cancer and the search for new cancer-associated genes. *Nature* 2013;499:214-8.
14. Lee W, Teckie S, Wiesner T, *et al.* PRC2 is recurrently inactivated through EED or SUZ12 loss in malignant peripheral nerve sheath tumors. *Nat Genet* 2014;46:1227-32.
15. Zhang M, Wang Y, Jones S, *et al.* Somatic mutations of SUZ12 in malignant peripheral nerve sheath tumors. *Nat Genet* 2014;46:1170-2.
16. Hirbe AC, Dahiya S, Miller CA, *et al.* Whole exome sequencing reveals the order of genetic changes during malignant transformation and metastasis in a single patient with NF1-plexiform neurofibroma. *Clin Cancer Res* 2015;21:4201-11.
17. Bottillo I, Ahlquist T, Brekke H, *et al.* Germline and somatic NF1 mutations in sporadic and NF1-associated malignant peripheral nerve sheath tumours. *J Pathol* 2009;217:693-701.

18. Verdijk RM, den Bakker MA, Dubbink HJ, *et al.* TP53 mutation analysis of malignant peripheral nerve sheath tumors. *J Neuropathol Exp Neurol* 2010;69:16-26.
19. Dubbink HJ, Bakels H, Post E, *et al.* TERT promoter mutations and BRAF mutations are rare in sporadic, and TERT promoter mutations are absent in NF1-related malignant peripheral nerve sheath tumors. *J Neurooncol* 2014;120:267-72.
20. Vogelstein B, Lane D, Levine AJ. Surfing the p53 network. *Nature* 2000;408:307-10.
21. Nigro JM, Baker SJ, Preisinger AC, *et al.* Mutations in the p53 gene occur in diverse human tumour types. *Nature* 1989;342:705-8.
22. Cichowski K, Shih TS, Schmitt E, *et al.* Mouse models of tumor development in neurofibromatosis type 1. *Science* 1999;286:2172-6.
23. Vogel KS, Klesse LJ, Velasco-Miguel S, *et al.* Mouse tumor model for neurofibromatosis type 1. *Science* 1999;286:2176-9.
24. Zhang Y, Xiong Y, Yarbrough WG. ARF promotes MDM2 degradation and stabilizes p53: ARF-INK4a locus deletion impairs both the Rb and p53 tumor suppression pathways. *Cell* 1998;92:725-34.
25. NCBI Pubmed. Available at: <https://www.ncbi.nlm.nih.gov/pubmed/>. Accessed Feb 13 2017.
26. Fletcher DM, Bridge JA, Hogendoorn PC, *et al.* WHO Classification of Tumours of Soft Tissue and Bone. Chapter: Malignant peripheral nerve sheath tumour (autors: Nielsen GP, Antonescu CR, Lothe RA). 2013;4th edition:187-89.
27. Karamchandani JR, Nielsen TO, van de Rijn M, *et al.* Sox10 and S100 in the diagnosis of soft-tissue neoplasms. *Appl Immunohistochem Mol Morphol* 2012;20:445-50.
28. Miettinen MM, Antonescu CR, Fletcher CDM, *et al.* Histopathologic evaluation of atypical neurofibromatous tumors and their transformation into malignant peripheral nerve sheath tumor in patients with neurofibromatosis 1-a consensus overview. *Hum Pathol* 2017;67:1-10.
29. Nonaka D, Chiriboga L, Rubin BP. Differential expression of S100 protein subtypes in malignant melanoma, and benign and malignant peripheral nerve sheath tumors. *J Cutan Pathol* 2008;35:1014-9.

30. Schaefer IM, Fletcher CD, Hornick JL. Loss of H3K27 trimethylation distinguishes malignant peripheral nerve sheath tumors from histologic mimics. *Mod Pathol* 2016;29:4-13.
31. Cleven AH, Sanna GA, Briaire-de Bruijn I, *et al.* Loss of H3K27 tri-methylation is a diagnostic marker for malignant peripheral nerve sheath tumors and an indicator for an inferior survival. *Mod Pathol* 2016;29:582-90.
32. Wang K, Li M, Hadley D, *et al.* PennCNV: an integrated hidden Markov model designed for high-resolution copy number variation detection in whole-genome SNP genotyping data. *Genome Res* 2007;17:1665-74.
33. PennCNV Affy. Protocol for CNV detection in Affymetrix SNP arrays. [Internet] Available from: http://www.openbioinformatics.org/penncnv/penncnv_tutorial_affy_gw6.html. Accessed Mar 20 2017.
34. Sveen A, Loes IM, Alagaratnam S, *et al.* Intra-patient Inter-metastatic Genetic Heterogeneity in Colorectal Cancer as a Key Determinant of Survival after Curative Liver Resection. *PLoS genetics* 2016;12:e1006225.
35. McCarroll SA, Kuruville FG, Korn JM, *et al.* Integrated detection and population-genetic analysis of SNPs and copy number variation. *Nat Genet* 2008;40:1166-74.
36. Van Loo P, Nordgard SH, Lingjaerde OC, *et al.* Allele-specific copy number analysis of tumors. *Proc Natl Acad Sci U S A* 2010;107:16910-5.
37. Beroukhi R, Getz G, Nghiemphu L, *et al.* Assessing the significance of chromosomal aberrations in cancer: methodology and application to glioma. *Proc Natl Acad Sci U S A* 2007;104:20007-12.
38. Mermel CH, Schumacher SE, Hill B, *et al.* GISTIC2.0 facilitates sensitive and confident localization of the targets of focal somatic copy-number alteration in human cancers. *Genome Biol* 2011;12:R41.
39. Nilsen G, Liestol K, Van Loo P, *et al.* Copynumber: Efficient algorithms for single- and multi-track copy number segmentation. *BMC Genomics* 2012;13:591.
40. Hanzelmann S, Castelo R, Guinney J. GSEA: gene set variation analysis for microarray and RNA-seq data. *BMC Bioinformatics* 2013;14:7.
41. IARC TP53 Database. Data file "somaticMutationsIARC TP53 Database, R18.txt". [Internet] Available from: <http://p53.iarc.fr/TP53SomaticMutations.aspx>. Accessed Feb 1 2017.

42. ExAC Browser. Variant: 17:7579472 G/C. [Internet] Available from: <http://exac.broadinstitute.org/variant/17-7579472-G-C>. Accessed Mar 27 2017.
43. Miller LD, Smeds J, George J, *et al.* An expression signature for p53 status in human breast cancer predicts mutation status, transcriptional effects, and patient survival. *Proc Natl Acad Sci U S A* 2005;102:13550-5.
44. Lothe RA, Smith-Sorensen B, Hektoen M, *et al.* Biallelic inactivation of TP53 rarely contributes to the development of malignant peripheral nerve sheath tumors. *Genes Chromosomes Cancer* 2001;30:202-6.
45. Rivlin N, Brosh R, Oren M, *et al.* Mutations in the p53 tumor suppressor gene: important milestones at the various steps of tumorigenesis. *Genes Cancer* 2011;2:466-74.
46. Rahrman EP, Moriarity BS, Otto GM, *et al.* Trp53 haploinsufficiency modifies EGFR-driven peripheral nerve sheath tumorigenesis. *Am J Pathol* 2014;184:2082-98.
47. Brosius SN, Turk AN, Byer SJ, *et al.* Neuregulin-1 overexpression and Trp53 haploinsufficiency cooperatively promote de novo malignant peripheral nerve sheath tumor pathogenesis. *Acta Neuropathol* 2014;127:573-91.
48. Pogribny IP, James SJ. Reduction of p53 gene expression in human primary hepatocellular carcinoma is associated with promoter region methylation without coding region mutation. *Cancer Lett* 2002;176:169-74.
49. Almeida LO, Custodio AC, Pinto GR, *et al.* Polymorphisms and DNA methylation of gene TP53 associated with extra-axial brain tumors. *Genetics and molecular research : GMR* 2009;8:8-18.
50. Chmelarova M, Krepinska E, Spacek J, *et al.* Methylation in the p53 promoter in epithelial ovarian cancer. *Clin Transl Oncol* 2013;15:160-3.
51. Amatya VJ, Naumann U, Weller M, *et al.* TP53 promoter methylation in human gliomas. *Acta Neuropathol* 2005;110:178-84.
52. Feber A, Wilson GA, Zhang L, *et al.* Comparative methylome analysis of benign and malignant peripheral nerve sheath tumors. *Genome Res* 2011;21:515-24.
53. Rieske P, Bartkowiak JK, Szadowska AM, *et al.* A comparative study of P53/MDM2 genes alterations and P53/MDM2 proteins immunoreactivity in soft-tissue sarcomas. *J Exp Clin Cancer Res* 1999;18:403-16.

54. Wallander ML, Tripp S, Layfield LJ. MDM2 amplification in malignant peripheral nerve sheath tumors correlates with p53 protein expression. *Arch Pathol Lab Med* 2012;136:95-9.
55. Holtkamp N, Atallah I, Okuducu AF, *et al.* MMP-13 and p53 in the progression of malignant peripheral nerve sheath tumors. *Neoplasia* 2007;9:671-7.
56. Kolberg M, Bruun J, Murumagi A, *et al.* Drug sensitivity and resistance testing identifies PLK1 inhibitors and gemcitabine as potent drugs for malignant peripheral nerve sheath tumors. *Mol Oncol* 2017;11:1156-71.
57. Xie Y, Wang A, Lin J, *et al.* Mps1/TTK: a novel target and biomarker for cancer. *J Drug Target* 2017;25:112-8.
58. Murahashi M, Hijikata Y, Yamada K, *et al.* Phase I clinical trial of a five-peptide cancer vaccine combined with cyclophosphamide in advanced solid tumors. *Clin Immunol* 2016;166-167:48-58.
59. Bradford D, Kim A. Current treatment options for malignant peripheral nerve sheath tumors. *Curr Treat Options Oncol* 2015;16:328.

Figure legends

Figure 1 Literature survey flow diagram. ^aSearch string on NCBI PubMed: “(tp53 OR p53)

AND (mpnst OR (malignant peripheral nerve sheath) OR neurofibrosarcomas OR neurofibrosarcoma OR (malignant schwannomas) OR (malignant schwannoma) OR neurosarcoma OR neurosarcomas) AND (mutation or mutations or polymorphism)”;

^bPublications not captured by the search string; ^cTwo of the 31 publications had overlapping tumor material and were merged into one study before calculations; ^dThe present study

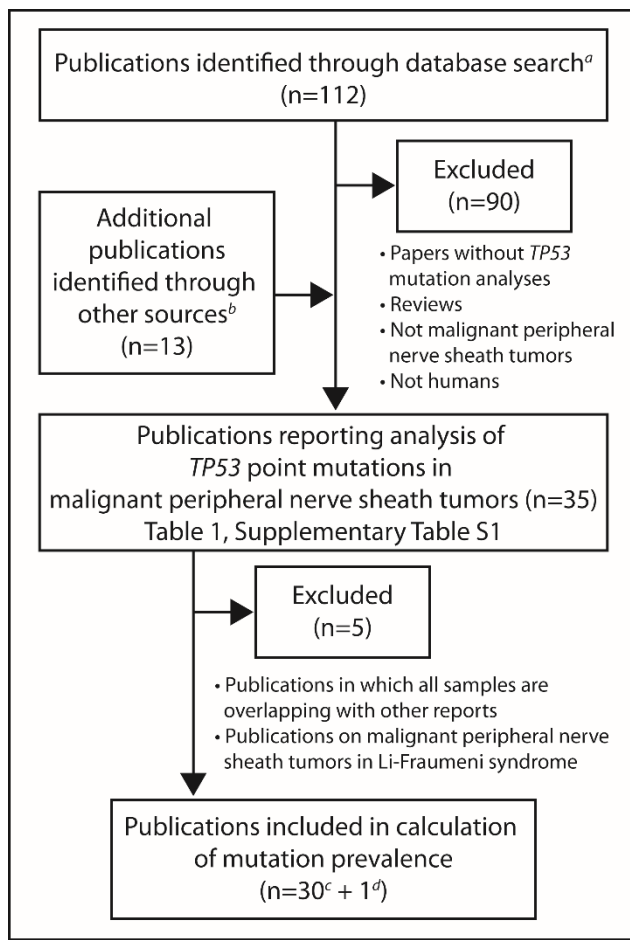


Figure 2 Genetic aberrations in *TP53* and *MDM2* identified in malignant peripheral nerve sheath tumors. **(a)** Exon/intron distribution of mutations. Diamond shaped (◆): 76 *TP53* mutations identified in malignant peripheral nerve sheath tumors from 74 patients from the literature (4 patients with Li-Fraumeni syndrome). Triangle shaped (▲): 9 mutations from 8 malignant peripheral nerve sheath tumors identified in this study. Star shaped (*): identified polymorphisms. **(b)** Mutations and polymorphisms identified in the present study. Polymorphisms were identified in malignant peripheral nerve sheath tumors from more than one patient, numbers are given in parentheses, c.108G>A and c.993+12T>C were found in overlapping samples. **(c)** Color coding for the different mutation types and pie chart showing the percentage of mutation types identified from the literature and the present study. **(d)** Overview of patients (numbers given in parentheses), clinical data, and genetic aberrations

found in *TP53* and *MDM2*. One malignant peripheral nerve sheath tumor had both a mutation and a polymorphism. For patients where more than one malignant tumor was analyzed only the primary or second primary tumor is given. Copy number is relative to the genome-wide median copy number state ($nAB \div \text{median copy number}$). Gain of ≥ 5 is defined as amplification (range: 5-23). Minimal region of overlap with copy number aberration: 61.3kB for *TP53* (chr17: 7,542,659-7,603,944); 396kB for *MDM2* (chr12: 69,127,774-69,523,923). Minimal region of loss of heterozygosity covering the *TP53* locus: 11.4MB, 4170 single nucleotide polymorphism probes.

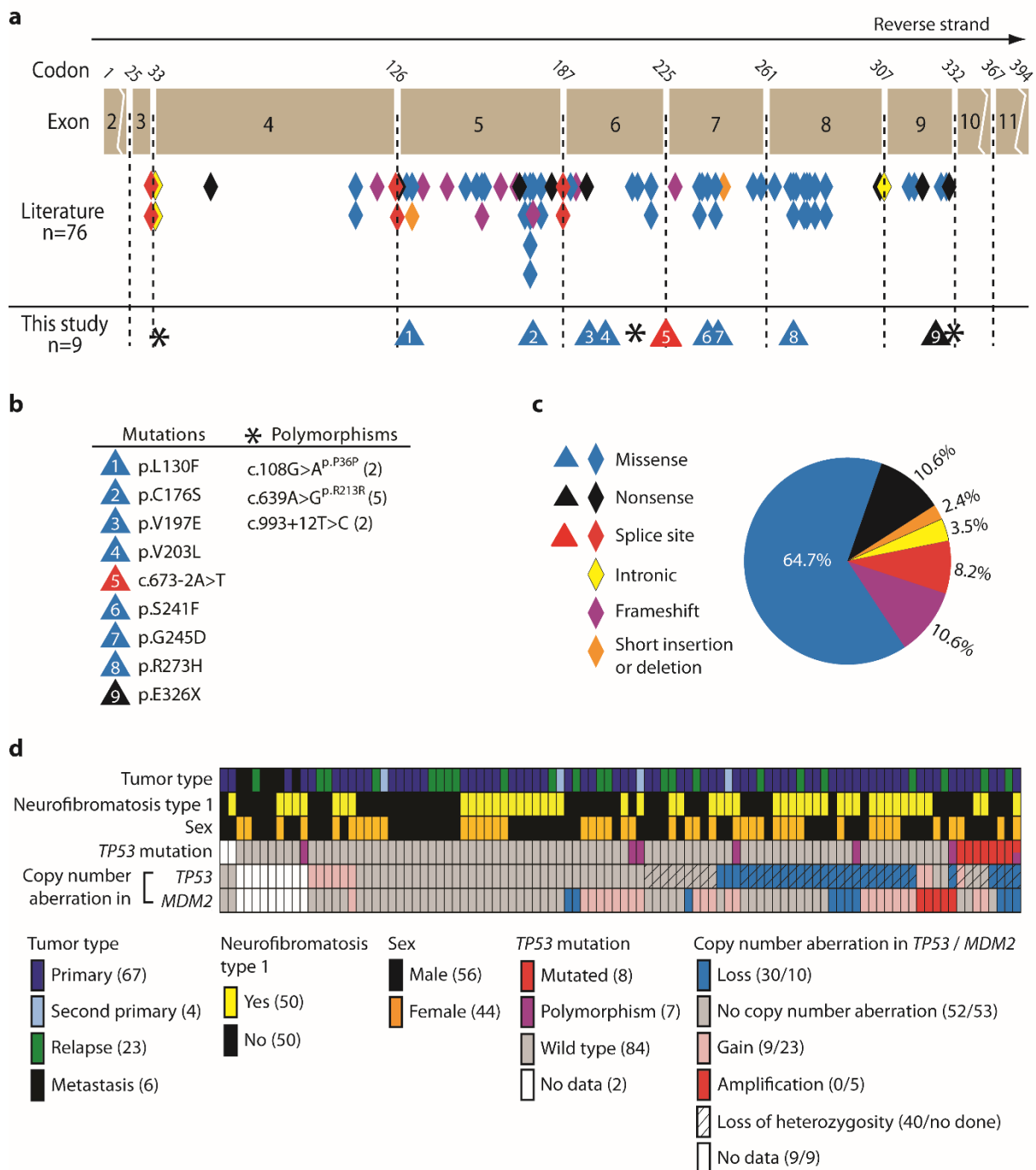


Figure 3 Dysregulation of the TP53 network in malignant peripheral nerve sheath tumors and association to patient survival. **(a)** Kaplan-Meier curves for patients in different molecular subgroups, for all patients (n=81) and **(b)** patients in complete remission (n=57). Hazard ratios, 95% confidence intervals (in brackets), and *P*-values are from Wald test. **(c)** Color codes for the different subgroups. **(d)** Box plot illustrating the difference in gene set score for

each molecular subgroup, *P*-values from Mann–Whitney–Wilcoxon exact test. (e) Heatmap shows the expression of the 15 genes in the gene set for each individual sample (n=63, log₂ expression values for each gene are scaled to mean 0 and standard deviation 1, samples are sorted according to the gene set score). The graph above the heatmap shows the Kernel density estimation curve and histogram for the amounts of samples with the given gene set score, a vertical line is drawn at the minimum point of the density curve (-0.12). (f) Kaplan-Meier curves for patients with a high (≥ -0.12) and low (< -0.12) gene set score.

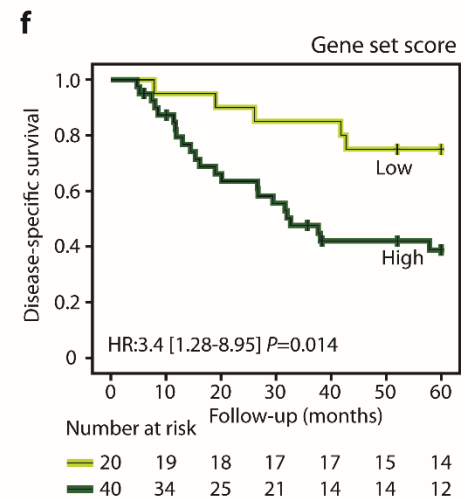
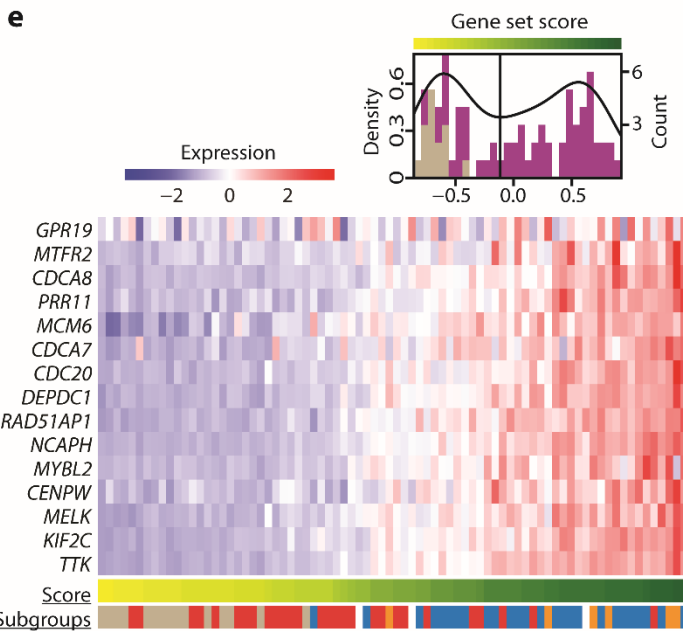
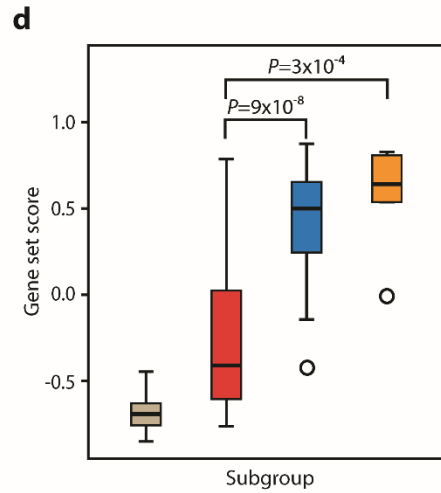
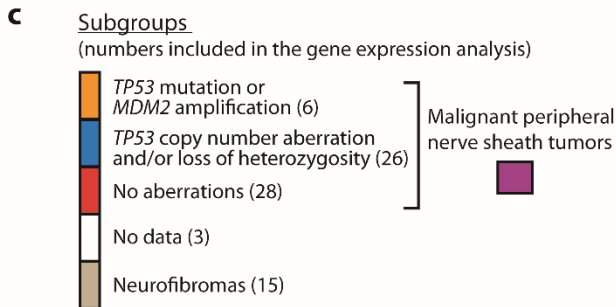
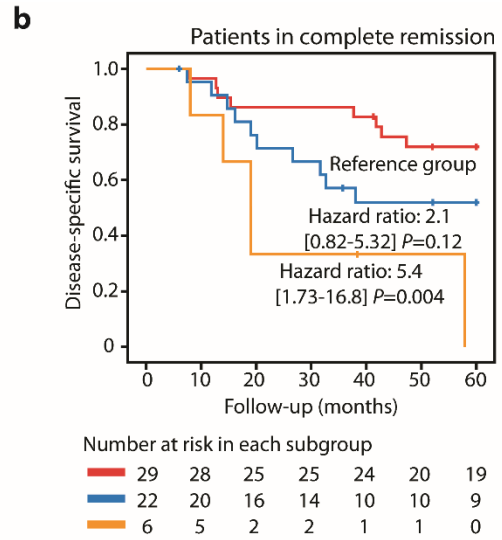
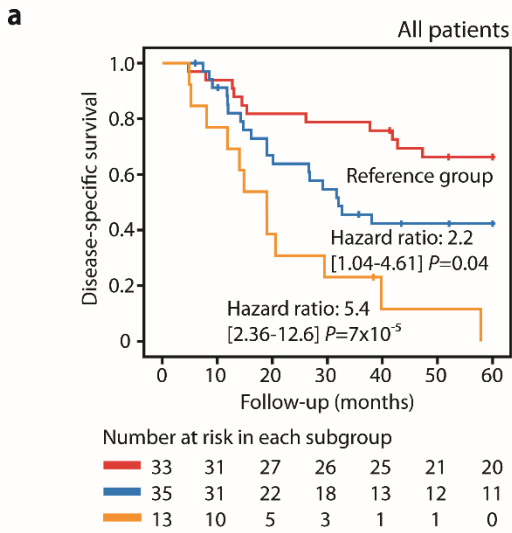


Table 1 Literature survey of *TP53* mutation analysis in malignant peripheral nerve sheath tumors

Year	First author	Method	Sample type	Exons analyzed	Number of tumors	Number of tumors	% with mutation ^f
1989	Nigro	PCR and ds	biopsy/cell line ^d	2 to 11	1	1	100
1990	Menon	PCR and bds	fresh frozen	5 to 8	1	7	14.3
1993	Boman	PCR-SSCP and ds	fresh frozen	2 to 11	0	1	0
1993	Lothe ^a	PCR CDGE and ds	fresh frozen	5,7,8	0	1	
1994	Flørenes	PCR-SSCP and ds	fresh frozen	5, 7, 8	0	3	0
1994	Latres	PCR-SSCP and ds	fresh frozen	2 to 9	0	6	0
1994	Legius	PCR and solid phase ds	fresh frozen/cell line ^d	4 to 9	2	3	66.7
1995	Castresana	PCR-SSCP and ds	fresh frozen	5 to 8	1	9	11.1
1995	Lothe ^a	PCR CDGE and ds	fresh frozen	5 to 8	0	7	
1997	Schneider-Stock ^b	PCR-SSCP and ds	fresh frozen	5 to 8	4 (3,1)	18 (10,12)	22.2
2002	Mawrin ^b	PCR-SSCP and ds	fresh frozen	5 to 8	4 (3,1)	18 (10,12)	22.2
1998	Taubert	PCR-SSCP and ds	fresh frozen/formalin-fixed	4 to 9	0	28	0
1999	Rieske	PCR-SSCP and ds	fresh frozen	5 to 8	2	15	13.3
2000	Rasmussen	PCR-SSCP and ds	not given	4 to 9	0	5	0
2000	Sonobe	PCR and ds	cell line ^d	4 to 9	1	1	100
2001	Birindelli	PCR-SSCP and ds	formalin-fixed	5 to 8	7	27	25.9
2001	Lefevre	PCR and ds	fresh frozen	2 to 11	1	1	100
2001	Leroy	PCR-DGGE and ds	fresh frozen	5 to 8	4	6	66.7
2001	Lothe ^a	PCR-DG/GE/TGGE and ds	fresh frozen	2 to 11	0	16	
2001	Watanabe	PCR-SSCP and ds	formalin-fixed	5 to 8	0	17	0
2002	Shin	PCR and ds	formalin-fixed	5 to 8	1	1	100
2004	Magrini	PCR and ds	fresh frozen	4 to 10	1	1	100
2004	Upadhyaya	PCR-SSCP and ds	not given	4 to 9	0	6	0
2007	Chao ^c	PCR and ds	leukocytes	4 to 10	1	1	
2007	Holtkamp	PCR-SSCP and ds	fresh frozen/formalin-fixed	1 to 11	4	36	11.1
2008	Upadhyaya	PCR and ds	not given	4 to 9	4	15	26.7
2009	Fauth	PCR and ds	formalin-fixed	2 to 11	1	2	50.0
2010	Verdijk	PCR and bds	formalin-fixed	4 to 9	17	72	23.6
2011	Beert	PCR and bds	cell line ^d	2 to 9	3	6	50.0
2012	Evans ^c	not given	not given	not given	3	3	
2014	Lee	WGS(n=15)/TS(n=31)	fresh frozen/formalin-fixed ^g	Full	11	46	23.9
2014	Zhang	WGS(n=4)/WES(n=4)	fresh frozen	Full	1	8	12.5
2015	Hirbe	WES/TS	fresh frozen/formalin-fixed	Full	3	16	18.8
2015	McPherson	WES	fresh frozen	Full	0	1	0
2017	Sohier	WES	fresh frozen	Full	0	8	0
2018	Høland ^a	PCR and ds	fresh frozen	2 to 11	8	98	8.2

References for all articles are included in Supplementary Table S1

Abbreviations: PCR, polymerase chain reaction; ds, direct sequencing; bds, bidirectional sequencing; CDGE, constant denaturing gel electrophoresis; SSCP, single-strand conformation polymorphism; DGGE, denaturing gradient gel electrophoresis; TGGE, Temperature gradient gel electrophoresis; WGS, whole genome sequencing; WES, whole exome sequencing; TS, targeted sequencing

^aFour publications with overlapping patient material, all patients were included in the present study (Høland, 2018)

^bTwo publications with overlapping patient material that were merged into one study, patients that could be verified as overlapping were excluded from calculations. Tumors analyzed in each study are given in parentheses

^cPublications analyzing tumors in patients with Li-Fraumeni syndrome, not included in calculations of mutation prevalence

^dCell lines, in Nigro 1989, 88-3/14; in Legius 1994, NF88-2, NF89-11, NF90-8; in Sonobe 2000, HS-SCH-2 (established in study); in Beert, HM1-3, HM9, and HM22-23 (established in study)

^eTumors from unique patients: each patient was only counted once as long as the information was available

^fOnly given for studies included in calculations of overall mutation prevalence

^gWGS samples were frozen while TS samples were formalin-fixed

Table 2 Clinical parameters for the malignant peripheral nerve sheath tumor patient cohort

Clinical parameter	Patients (n=100)
Neurofibromatosis type 1 ^a	
No	50
Yes	50
Sex	
Male	56
Female	44
Age at diagnosis ^c	
Median (range)	36 (11-82)
Location	
Extremities	70
Non-extremities	29
Not available	1
Tumor size (cm) ^c	
Median (range)	10 (3-34)
Complete remission ^{b,c}	
Yes	65
No	17
Not available	18
Grade ^d	
Low	7
High	90
Not available	3
Survival	
Median survival time (months)	42.7
Number of events	60
Survival data available	96 ^f
Lost to follow up	4
Tumors analyzed	
Primaries	72
Relapses	25
Metastases	8
<i>TP53</i> mutation or <i>MDM2</i> amplification	
None	76
<i>TP53</i> point mutation	8
<i>MDM2</i> amplification ^e	5
Not available	11

^aTwo of the included tumors were triton tumors, one from a patient with neurofibromatosis type 1 and one sporadic.

^bPatients in complete remission had wide or marginal surgical margins after removal of the primary tumor and no metastasis at diagnosis, while those not in complete remission had intralesional margins and/or metastasis at diagnosis

^cRefers to the initial primary tumor, tumor size is the maximum tumor diameter

^dGrade is given for the initial primary tumor, except for 3 high grade and 2 low cases, where the grade of the analyzed tumor is given (relapse or second primary)

^eAmplification is defined as gain of ≥ 5 copies relative to the median genome wide copy number

^fOnly 86 patients, from whom a primary or a local relapse were analyzed, were included in survival analyses with molecular markers, see Supplementary Table S2 for details.

Table 3 Survival analysis for patients with malignant peripheral nerve sheath tumor

Clinical parameter	Categories	Univariable			Multivariable			
		N	% survival ^c (standard error)	P-value ^d	Hazard ratio (95% confidence interval)	N	P-value ^d	Hazard ratio (95% confidence interval)
Neurofibromatosis type 1	No	44	55.1 (7.7)	Ref		37	Ref	
	Yes	42	35.6 (7.7)	0.06	1.79 (0.99-3.23)	33	0.78	0.90 (0.41-1.96)
Sex	Male	49	48.4 (7.2)	Ref		37	Ref	
	Female	37	41.8 (8.2)	0.41	1.28 (0.71-2.30)	33	0.97	1.02 (0.47-2.21)
Age at diagnosis ^{a,b}		86		0.99	1.00 (0.98-1.02)	70	0.15	0.98 (0.96-1.01)
Location	Extremities	63	53.4 (6.5)	Ref		54	Ref	
	Non-extremities	23	26.6 (9.6)	0.02	2.05 (1.11-3.78)	16	0.34	1.51 (0.65-3.54)
Tumor size ^{a,b}		83		0.01	1.06 (1.01-1.11)	70	0.03	1.06 (1.01-1.12)
Complete remission ^{a,e}	Yes	61	57.4 (6.5)	Ref		56	Ref	
	No	14	7.9 (7.5)	4.1x10⁻⁵	4.51 (2.29-9.25)	14	0.002	3.71 (1.63-8.46)
TP53 mutation or MDM2 amplification	No	68	54.3 (6.2)	Ref		60	Ref	
	Yes	13	0 (58) ^f	3.0x10⁻⁴	3.52 (1.78-6.98)	10	0.01	3.39 (1.38-8.33)

^aRefers to the initial primary tumor, tumor size is the maximum tumor diameter (cm)

^bContinuous variable

^cCumulative Proportion Surviving

^dP-values from Wald test, Cox regression, for five years disease specific survival

^ePatients in complete remission had wide or marginal surgical margins after removal of the primary tumor and no metastasis at diagnosis, while those not in complete remission had intralesional margins and/or metastasis at diagnosis

^fFor groups with no survivors, the value in parentheses indicates months of the last disease specific death

Values written in bold phase indicate significant findings